

Synthesis and Investigation of $[\text{Cp}^*(\text{PMe}_3)\text{Rh}(\text{H})(\text{H}_2)]^+$ and Its Partially Deuterated and Tritiated Isotopomers: Evidence for a Hydride/Dihydrogen Structure

Felicia L. Taw,[†] Heather Mellows,[‡] Peter S. White,[†] Frederick J. Hollander,[§]
Robert G. Bergman,^{*,§} Maurice Brookhart,^{*,†} and D. Michael Heinekey^{*,‡}

Contribution from the Department of Chemistry, University of North Carolina at Chapel Hill, CB #3290, Chapel Hill, North Carolina 27599-3290, Department of Chemistry, University of Washington, Box 351700, Seattle, Washington 98195-1700, and Department of Chemistry, University of California and Division of Chemical Sciences, Lawrence Berkeley National Laboratory, Berkeley, California 94720

Received July 12, 2001

Abstract: Hydrogenolysis of $[\text{Cp}^*(\text{PMe}_3)\text{Rh}(\text{Me})(\text{CH}_2\text{Cl}_2)]^+\text{BAR}'_4^-$ (**4**, $\text{Ar}' = 3,5\text{-C}_6\text{H}_3(\text{CF}_3)_2$) in dichloromethane afforded the nonclassical polyhydride complex $[\text{Cp}^*(\text{PMe}_3)\text{Rh}(\text{H})(\text{H}_2)]^+\text{BAR}'_4^-$ (**1**), which exhibits a single hydride resonance at all accessible temperatures in the ^1H NMR spectrum. Exposure of solutions of **1** to D_2 or T_2 gas resulted in partial isotopic substitution in the hydride sites. Formulation of **1** as a hydride/dihydrogen complex was based upon T_1 ($T_1(\text{min}) = 23$ ms at 150 K, 500 MHz), $J_{\text{H-D}}$ (ca. 10 Hz), and $J_{\text{H-T}}$ (ca. 70 Hz) measurements. The barrier (ΔG^\ddagger) to exchange of hydride with dihydrogen sites was determined to be less than ca. 5 kcal/mol. Protonation of $\text{Cp}^*(\text{PMe}_3)\text{Rh}(\text{H})_2$ (**2**) using $\text{H}(\text{OEt}_2)_2\text{BAR}'_4$ resulted in binuclear species $[(\text{Cp}^*(\text{PMe}_3)\text{Rh}(\text{H}))_2(\mu\text{-H})]^+\text{BAR}'_4^-$ (**3**), which is formed in a reaction involving **1** as an intermediate. Complex **3** contains two terminal hydrides and one bridging hydride ligand which exchange with a barrier of 9.1 kcal/mol as observed by ^1H NMR spectroscopy. Additionally, the structures of **3** and **4**, determined by X-ray diffraction, are reported.

Introduction

The study of transition metal polyhydrides comprises a large portion of organometallic chemistry.¹ In particular, these polyhydride complexes play a prominent role in many homogeneous catalytic processes, including hydrogenation of unsaturated bonds.² Such complexes have been shown to adopt both classical structures with terminal hydride ligands and nonclassical structures containing one or more $\eta^2\text{-H}_2$ ligands. The first classical polyhydride, $\text{Fe}(\text{H})_2(\text{CO})_4$, was discovered by Hieber in 1931.³ However, it was not until 1984 that Kubas reported the first stable nonclassical dihydrogen complex, $\text{W}(\text{CO})_3(\text{P}^i\text{-Pr}_3)_2(\text{H}_2)$.⁴

A concise summary of the standard bonding schemes for metal–dihydrogen and metal–hydride bonds has been offered by Crabtree.⁵ Metal–dihydrogen interactions involve donation

of H_2 σ electrons to an empty metal d_σ orbital balanced by back-donation of metal d_π electrons to the H_2 σ^* orbital. Excessive back-donation into the H_2 σ^* orbital leads to scission of the H–H bond and thus formation of terminal hydride species.

The factors determining which structure is adopted in a particular case are not well understood. Since transition metals generally form stronger M–H bonds upon descending a column of the periodic table, classical hydride structures are favored for 5d metals. Specifically, a comparison of 4d vs 5d metals with similar co-ligands indicates that the second row metal is often a dihydrogen complex while the third row metal prefers the dihydride structure. Numerous examples from the literature support this idea, such as $\text{Tp}^*\text{Rh}(\text{H})_2(\text{H}_2)$ ⁶ vs Tp^*IrH_4 ⁷ ($\text{Tp}^* = \text{HB}(3,5\text{-Me}_2\text{pz})_3$),⁸ $[\text{CpRu}(\text{P}-\text{P})(\text{H}_2)]^+$ ⁹ vs $[\text{CpOs}(\text{P}-\text{P})(\text{H}_2)]^+$ ¹⁰ ($\text{P}-\text{P} = \text{dppe}$, dppp), and $(\text{PCy}_3)_2\text{Ru}(\text{H})_2(\text{H}_2)$ ¹¹ vs $(\text{P}^i\text{Pr}_2\text{Ph})_2\text{Os}(\text{H})_6$.¹² However, exceptions exist in which both second-

[†] University of North Carolina at Chapel Hill.

[‡] University of Washington.

[§] University of California and Division of Chemical Sciences.

- (1) Recent reviews: (a) Maseras, F.; Lledos, A.; Clot, E.; Eisenstein, O. *Chem. Rev.* **2000**, *100*, 601. (b) Sabo-Etienne, S.; Chaudret, B. *Chem. Rev.* **1998**, *98*, 2077. (c) Lin, Z.; Hall, M. B. *Coord. Chem. Rev.* **1994**, *135/136*, 845. (d) Heinekey, D. M.; Oldham, W. J., Jr. *Chem. Rev.* **1993**, *93*, 913. (e) Crabtree, R. H. *Angew. Chem., Int. Ed. Engl.* **1993**, *32*, 789. (f) Jessop, P. G.; Morris, R. H. *Coord. Chem. Rev.* **1992**, *121*, 155.
- (2) Esteruelas, M. A.; Oro, L. A. *Chem. Rev.* **1998**, *98*, 577.
- (3) Hieber, W.; Leutert, F. *Naturwissenschaften* **1931**, *19*, 360.
- (4) Kubas, G. J.; Ryan, R. R.; Swanson, B. I.; Vergamini, P. J.; Wasserman, H. J. *J. Am. Chem. Soc.* **1984**, *106*, 451.
- (5) Hamilton, D. G.; Crabtree, R. H. *J. Am. Chem. Soc.* **1988**, *110*, 4126 and references therein.

- (6) (a) Bucher, U. E.; Lengweiler, T.; Nanz, D.; von Philipsborn, W.; Venanzi, L. M. *Angew. Chem., Int. Ed. Engl.* **1990**, *29*, 548. (b) Nanz, D.; von Philipsborn, W.; Bucher, U. E.; Venanzi, L. M. *Magn. Reson. Chem.* **1991**, *29*, S38.
- (7) Paneque, M.; Poveda, M. L.; Taboada, S. *J. Am. Chem. Soc.* **1994**, *116*, 4519.
- (8) Trofimenko, S. *Chem. Rev.* **1993**, *93*, 943.
- (9) Conroy-Lewis, F. M.; Simpson, S. J. *J. Chem. Soc., Chem. Commun.* **1987**, 1675.
- (10) Jia, G.; Ng, W. S.; Yao, J.; Lau, C. P.; Chen, Y. *Organometallics* **1996**, *15*, 5039.
- (11) Borowski, A. F.; Donnadiu, B.; Daran, J. C.; Sabo-Etienne, S.; Chaudret, B. *Chem. Commun.* **2000**, 543.
- (12) Howard, J. A. K.; Johnson, O.; Koetzle, T. F.; Spencer, J. L. *Inorg. Chem.* **1987**, *26*, 2930.

third-row metal analogues with similar co-ligands adopt non-classical structures. Examples include the dihydrogen complexes $M(\text{CO})_3(\text{P}^i\text{Pr}_3)_2(\text{H}_2)$ ($M = \text{Mo}, \text{W}$),⁴ $[\text{Tp}(\text{PMe}_3)\text{M}(\text{H})(\text{H}_2)]^+$ ($M = \text{Rh}, \text{Ir}$),¹³ and $[\text{MCl}(\text{H}_2)(\text{depe})_2]^+$ ($M = \text{Ru}, \text{Os}$).¹⁴

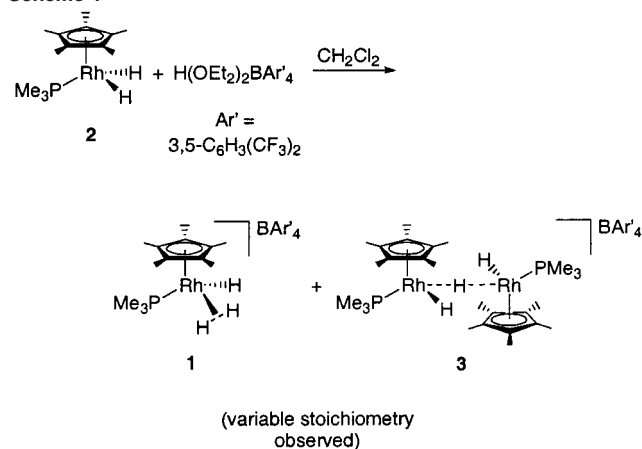
In these and other complexes, the choice of ligands around the metal center also plays a key role in defining structure. For example, Hay has calculated that replacing all the CO ligands with phosphines in $\text{W}(\text{CO})_3(\text{P}^i\text{Pr}_3)_2(\text{H}_2)$ will result in dihydride formation.¹⁵ The CO ligands serve as π -acceptors which stabilize filled metal d orbitals, thereby inhibiting excessive back-donation of metal d_π electrons to the H_2 σ^* orbital. This is consistent with the observation that $\text{W}(\text{CO})_3(\text{P}^i\text{Pr}_3)_2(\text{H}_2)$ contains a dihydrogen ligand but $\text{Mo}(\text{PMe}_3)_5(\text{H})_2$ ¹⁶ contains terminal hydrides.

Theoretical studies of the $\text{LRh}''\text{H}_4''$ ($L = \text{Cp}, \text{Tp}$) system suggest that when $L = \text{Cp}$ a classical tetrahydride structure is more stable, whereas if $L = \text{Tp}$ a nonclassical isomer is preferred.¹⁷ This difference in behavior can be rationalized by the observation that Cp is a stronger electron-donor toward Rh than Tp, thereby contributing more electron density to the H_2 antibonding σ^* orbital. In addition, the character of the Tp ligand causes octahedral geometries to be favored ($\text{TpRh}(\text{H})_2(\text{H}_2)$ is octahedral, whereas $\text{TpRh}(\text{H})_4$ is not), while Cp complexes can adopt three or four-legged piano-stool structures.¹⁷ For example, while $[\text{Cp}(\text{PMe}_3)\text{Ir}(\text{H})_3]^+$ ¹⁸ and $\text{Cp}^*(\text{PCy}_3)\text{Ru}(\text{H})_3$ ¹⁹ form classical polyhydrides, the Tp analogues, $[\text{Tp}(\text{PMe}_3)\text{Ir}(\text{H})(\text{H}_2)]^+$ ²⁰ and $\text{Tp}^*(\text{PCy}_3)\text{Ru}(\text{H})(\text{H}_2)$,²¹ contain $\eta^2\text{-H}_2$ ligands. However, inconsistencies in this pattern exist which cannot be easily explained. For instance, $\text{Cp}^*\text{Ir}(\text{H})_4$ ²² contains only terminal hydride ligands, as expected, but the Tp^* analogue $\text{Tp}^*\text{Ir}(\text{H})_4$ ²⁰ also seems to adopt a classical structure based upon chemical behavior and T_1 measurements.

The Ir(V) complex $[\text{Cp}(\text{PMe}_3)\text{Ir}(\text{H})_3]^+$ was shown by Heinekey in 1990 to be a classical trihydride exhibiting quantum mechanical exchange coupling between the hydrogen nuclei.¹⁸ The Cp^* analogue $[\text{Cp}^*(\text{PMe}_3)\text{Ir}(\text{H})_3]^+$, which was first characterized by Bergman²³ in 1985, was also shown by Heinekey²⁴ in 1996 to be a classical trihydride. This complex undergoes a rapid hydride permutation process which leads to a single hydride resonance in the ^1H NMR spectrum at temperatures above 220 K. At lower temperatures, two distinct hydride environments are observed. The classical structure of this compound is not surprising due to the presence of a Cp^* ligand in addition to being a third-row metal complex.

Herein, we describe the preparation and characterization of the rhodium analogue, $[\text{Cp}^*(\text{PMe}_3)\text{Rh}''\text{H}_3'']^+$ (no structure implied). From the previous discussion, it is not obvious which

Scheme 1



structure would be energetically favored. While the presence of electron-donating Cp^* and PMe_3 ligands might induce hydride formation, rhodium is a second-row metal which prefers lower oxidation states. Theoretical studies by Hall on the model complex $[\text{Cp}(\text{PH}_3)\text{Rh}''\text{H}_3'']^+$ suggested that the hydride/dihydrogen structure and the classical trihydride were very similar in energy, differing only by 0.5 kcal/mol.²⁵

Kubas has shown that partial substitution of deuterium in dihydrogen complexes allows direct measurement of $J_{\text{H-D}}$ values, which can be used to verify $\eta^2\text{-H}_2$ bonding.⁴ Similarly, Crabtree has shown that short T_1 times are also indicative of bound H_2 ligands, which display rapid dipole-dipole relaxation due to the short H-H distances.^{5,26} A combination of these techniques is used here, in addition to examination of partially tritiated complexes, to determine that $[\text{Cp}^*(\text{PMe}_3)\text{Rh}(\text{H})(\text{H}_2)]^+\text{BAR}'_4^-$ adopts a hydride/dihydrogen structure.

Additionally, synthesis and characterization of a binuclear rhodium hydride complex, $[(\text{Cp}^*(\text{PMe}_3)\text{Rh}(\text{H}))_2(\mu\text{-H})]^+\text{BAR}'_4^-$, is presented. The reaction to form this binuclear species involves as an intermediate the hydride/dihydrogen $[\text{Cp}^*(\text{PMe}_3)\text{Rh}(\text{H})(\text{H}_2)]^+\text{BAR}'_4^-$ complex mentioned above. The binuclear complex contains two terminal hydrides and one bridging hydride ligand which are exchanging as observed by ^1H NMR spectroscopy. The activation barrier for exchange of a terminal hydride with the bridging hydride has been determined by NMR line-broadening techniques.

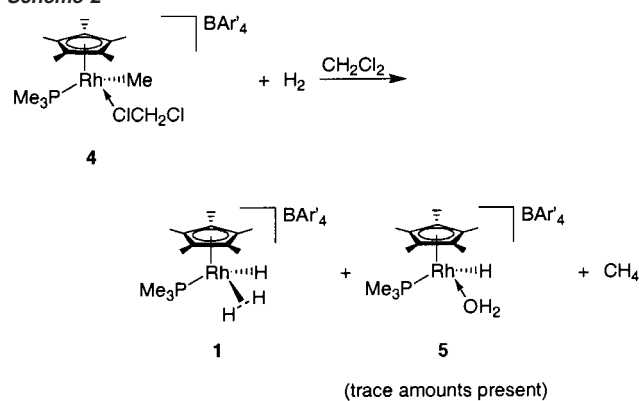
Results and Discussion

Generation of $[\text{Cp}^*(\text{PMe}_3)\text{Rh}(\text{H})(\text{H}_2)]^+\text{BAR}'_4^-$ (1). The rhodium hydride/dihydrogen species, formulated as $[\text{Cp}^*(\text{PMe}_3)\text{Rh}(\text{H})(\text{H}_2)]^+\text{BAR}'_4^-$ (1) on the basis of evidence presented below, has been prepared via two independent routes. Protonation of the previously reported neutral dihydride complex $\text{Cp}^*(\text{PMe}_3)\text{Rh}(\text{H})_2$ ²⁷ (2) using excess $\text{H}(\text{OEt}_2)_2\text{BAR}'_4$ (1–2 equiv) resulted in the formation of 1. However, this reaction occurred with concomitant formation of a side product, $[(\text{Cp}^*(\text{PMe}_3)\text{Rh}(\text{H}))_2(\mu\text{-H})]^+\text{BAR}'_4^-$ (3), which was present in significant amounts (Scheme 1; see below for characterization of 3). The use of 2 equiv of $\text{H}(\text{OEt}_2)_2\text{BAR}'_4$ led to product ratios of approximately 9:1 for formation of 1 versus 3, whereas protonation using 1 equiv resulted in product ratios of approximately 1:1.

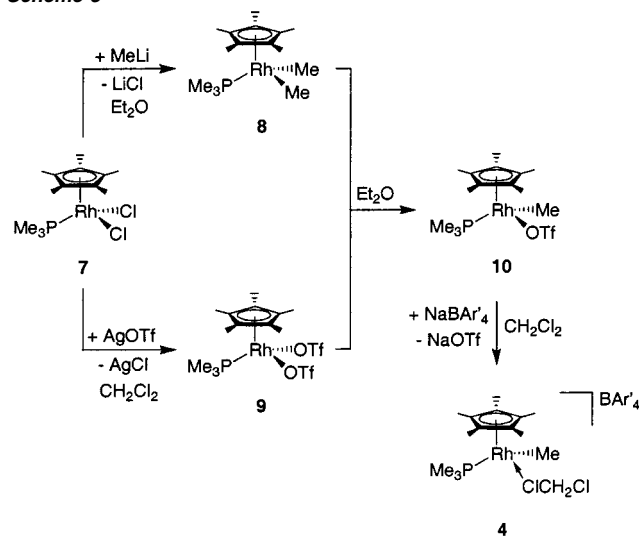
- (13) Oldham, W. J., Jr.; Hinkle, A. S.; Heinekey, D. M. *J. Am. Chem. Soc.* **1997**, *119*, 11028.
 (14) Cappellani, E. P.; Maltby, P. A.; Morris, R. H.; Schweitzer, C. T.; Steele, M. R. *Inorg. Chem.* **1989**, *28*, 4437.
 (15) Hay, P. J. *J. Am. Chem. Soc.* **1987**, *109*, 705.
 (16) Lyons, D.; Wilkinson, G.; Thornton-Pett, M.; Hursthouse, M. B. *J. Chem. Soc., Dalton Trans.* **1984**, 695.
 (17) Gelabert, R.; Moreno, M.; Lluch, J. M.; Lledós, A. *Organometallics* **1997**, *16*, 3805.
 (18) Heinekey, D. M.; Millar, J. M.; Koetzle, T. F.; Payne, N. G.; Zilm, K. W. *J. Am. Chem. Soc.* **1990**, *112*, 909.
 (19) Arliguie, T.; Chaudret, B. *J. Chem. Soc., Chem. Commun.* **1986**, *13*, 985.
 (20) Heinekey, D. M.; Oldham, W. J., Jr. *J. Am. Chem. Soc.* **1994**, *116*, 3137.
 (21) Moreno, B.; Sabo-Etienne, S.; Chaudret, B.; Rodriguez, A.; Jalon, F.; Trofimenko, S. *J. Am. Chem. Soc.* **1995**, *117*, 7441.
 (22) Gilbert, T. M.; Bergman, R. G. *Organometallics* **1983**, *2*, 1458.
 (23) Gilbert, T. M.; Bergman, R. G. *J. Am. Chem. Soc.* **1985**, *107*, 3502.
 (24) Heinekey, D. M.; Hinkle, A. S.; Close, J. D. *J. Am. Chem. Soc.* **1996**, *118*, 5353.

- (25) Lin, Z.; Hall, M. B. *Organometallics* **1992**, *11*, 3801.
 (26) Crabtree, R. H.; Lavin, M. *J. Chem. Soc., Chem. Commun.* **1985**, 1661.
 (27) Isobe, K.; Bailey, P. M.; Maitlis, P. M. *J. Chem. Soc., Dalton Trans.* **1981**, 2003.

Scheme 2



Scheme 3



Hydrogenolysis of the rhodium(III) dichloromethane adduct, $[\text{Cp}^*(\text{PMe}_3)\text{Rh}(\text{Me})(\text{CH}_2\text{Cl}_2)]^+\text{BAR}'_4^-$ (**4**), produced **1** in good yields (Scheme 2). In this reaction, small and variable amounts of a byproduct formulated as the aquo complex $[\text{Cp}^*(\text{PMe}_3)\text{Rh}(\text{H})(\text{OH}_2)]^+\text{BAR}'_4^-$ (**5**) were observed. The presence of any residual water caused displacement of the labile $\mu^2\text{-H}_2$ ligand from **1** to form **5**. Complex **1** has not been isolated, as rapid decomposition occurs upon removal of solvent even at low temperatures. Thus, for all experiments conducted in this report, **1** has been generated in situ by hydrogenolysis of **4**. Partial deuteration and tritiation of **1** were achieved by exposure of solutions of **1** to D_2 or T_2 gas.

Synthesis of $[\text{Cp}^*(\text{PMe}_3)\text{Rh}(\text{Me})(\text{CH}_2\text{Cl}_2)]^+\text{BAR}'_4^-$ (4**).** The cationic rhodium methyl complex **4** can be synthesized using procedures analogous to those employed for the previously reported iridium analogue, $[\text{Cp}^*(\text{PMe}_3)\text{Ir}(\text{Me})(\text{CH}_2\text{Cl}_2)]^+\text{BAR}'_4^-$ (**6**).²⁸ Excess MeLi was added to the known dichloride $\text{Cp}^*(\text{PMe}_3)\text{Rh}(\text{Cl})_2$ (**7**) to produce the dimethyl species $\text{Cp}^*(\text{PMe}_3)\text{Rh}(\text{Me})_2$ (**8**). Similarly, excess AgOTf was added to **7** to produce a bis-triflate complex $\text{Cp}^*(\text{PMe}_3)\text{Rh}(\text{OTf})_2$ (**9**).³⁰ Species **8** and **9** were then combined in equal amounts in a comproportionation reaction, resulting in conversion to the rhodium methyl triflate compound $\text{Cp}^*(\text{PMe}_3)\text{Rh}(\text{Me})(\text{OTf})$

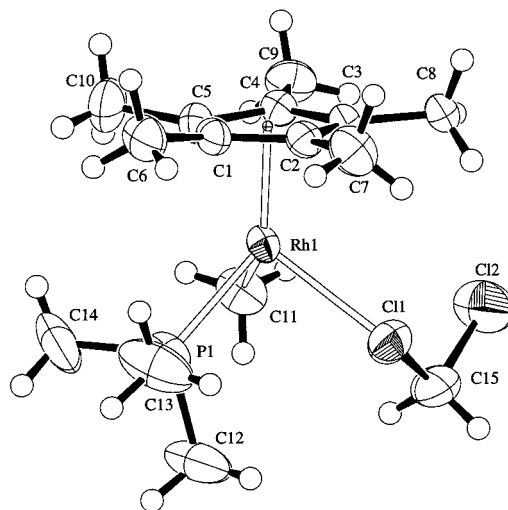


Figure 1. ORTEP diagram of $[\text{Cp}^*(\text{PMe}_3)\text{Rh}(\text{Me})(\text{CH}_2\text{Cl}_2)]^+$ (**4**, BAR'_4^- counterion omitted for clarity).

Scheme 4

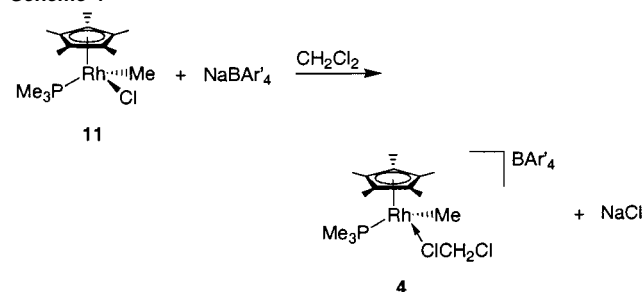


Table 1: Selected Bond Distances and Bond Angles

	bond distance (Å)		bond angle (deg)
Rh(1)–Cp*(centroid)	1.8620(4)	Cp*–Rh(1)–P(1)	132.03(4)
Rh(1)–P(1)	2.285(1)	Cp*–Rh(1)–C(11)	123.3(1)
Rh(1)–C(11)	2.106(5)	Cp*–Rh(1)–Cl(1)	122.23(3)
Rh(1)–Cl(1)	2.488(1)	P(1)–Rh(1)–C(11)	84.5(1)

(**10**). Exchange of triflate with the noncoordinating BAR'_4^- ligand to produce **4** was achieved by adding NaBAR'_4 to **10** using CH_2Cl_2 as solvent (Scheme 3).

We have since discovered that a more efficient synthesis of **4** involved addition of NaBAR'_4 to the previously reported compound $\text{Cp}^*(\text{PMe}_3)\text{Rh}(\text{Me})(\text{Cl})$ (**11**).³¹ A direct exchange of chloride ligand with BAR'_4^- occurred to produce **4** in high yields (Scheme 4). A clear advantage of this method is that it employs easily prepared, air-stable complex **11** to produce the air-sensitive compound **4** directly.

Orange-red crystals of **4**, which are thermally and air-sensitive, were isolated in approximately 80% yield and were fully characterized. An X-ray crystal structure of **4** is shown in Figure 1. Table 1 lists some selected bond distances and bond angles for this compound. Complex **4** forms a structure with a three-legged piano stool geometry. While two dichloromethane molecules are present per rhodium center in the crystal lattice, only one is within bonding distance (Rh–Cl distance = 2.49 Å) to the metal center. The other dichloromethane molecule and the tetraarylborate anion are clearly noncoordinating.

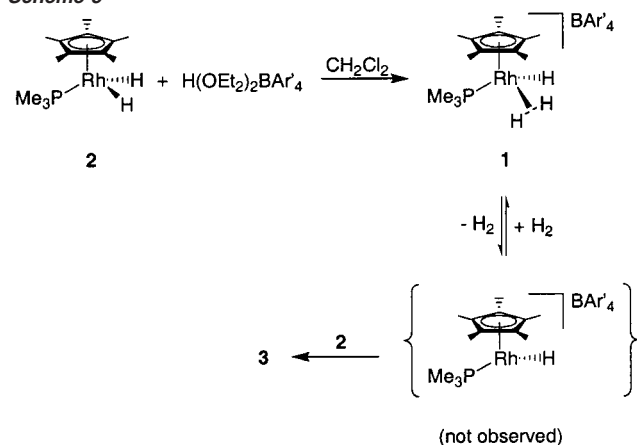
(28) Burger, P.; Bergman, R. G. *J. Am. Chem. Soc.* **1993**, *115*, 10462.

(29) Diversi, P.; Iaconi, S.; Ingrosso, G.; Laschi, F.; Lucherini, A.; Pinzino, C.; Uccello-Barretta, G.; Zanello, P. *Organometallics* **1995**, *14*, 3275.

(30) Stang, P. J.; Huang, Y. H.; Arif, A. M. *Organometallics* **1992**, *11*, 231.

(31) Jones, W. D.; Feher, F. J. *Organometallics* **1983**, *2*, 562.

Scheme 5



Synthesis and Characterization of $[(\text{Cp}^*(\text{PMe}_3)\text{Rh}(\text{H}))_2(\mu\text{-H})]^+\text{BAR}'_4^-$ (3**).** When excess $\text{H}(\text{OEt}_2)_2\text{BAR}'_4$ was added to **2** to generate rhodium hydride **1**, a second hydride species (**3**) was also produced (Scheme 1). After further studies, we found that the most efficient synthesis of complex **3** could be achieved by adding exactly 0.5 equiv of $\text{H}(\text{OEt}_2)_2\text{BAR}'_4$ to rhodium dihydride **2**. The mechanism presumably involves initial protonation of **2** to form hydride/dihydrogen species **1**. Reversible loss of H_2 occurs to produce a rhodium monohydride species (not observed), which can then combine with 1 equiv of **2** to produce the binuclear complex (Scheme 5). Observation by ^1H NMR spectroscopy of the initial formation and then disappearance of **1** as the reaction progresses, and the appearance of free H_2 in the product mixture, lend support to this mechanistic pathway. An X-ray crystal structure of **3** has been obtained; the ORTEP diagram is shown in Figure 2. The Rh–Rh distance of 2.94 Å is suggestive of a weak metal–metal interaction.

Although they were not located in the diffraction study, NMR analysis demonstrates that binuclear rhodium complex **3** contains two terminal hydride ligands and one bridging hydride moiety. These hydrides exchange rapidly at room temperature and exhibit fluxional behavior as observed by variable-temperature ^1H NMR spectroscopy. At 313 K, the hydride resonance appears as a well-resolved triplet of triplets due to averaged coupling to two rhodium nuclei and two phosphorus nuclei ($\delta -16.99$ ppm; $^1J_{\text{Rh-H}} = 14.4$ Hz, $^2J_{\text{P-H}} = 20.0$ Hz). Upon lowering the temperature the resonance broadens significantly. At 223 K, the hydride resonance is distinguishable only as a structureless lump above the baseline. Upon further cooling, decoalescence occurs to reveal two distinct hydride resonances that integrate in a 2:1 ratio. At temperatures below 203 K the ^1H NMR signal for the two equivalent terminal hydrides was easily distinguishable from the signal for the bridging hydride. Unlike the hydride region, the alkyl region varied little with temperature.

Werner has reported a similar rhodium complex, $[(\text{Cp}(\text{P}^i\text{Pr}_3)\text{Rh})_2(\mu\text{-H})_3]^+\text{PF}_6^-$ (**12**), which was synthesized by protonation of $\text{Cp}(\text{P}^i\text{Pr}_3)\text{Rh}(\text{H})_2$ (**13**) using $\text{CF}_3\text{CO}_2\text{H}$.³² From NMR data obtained at room temperature, complex **12** was rationalized as a binuclear species containing three equivalent bridging hydride ligands. It is likely that the structure of **12** is similar to **3** and contains only one bridging hydrogen, but to date no low-temperature NMR studies have been reported to clarify this

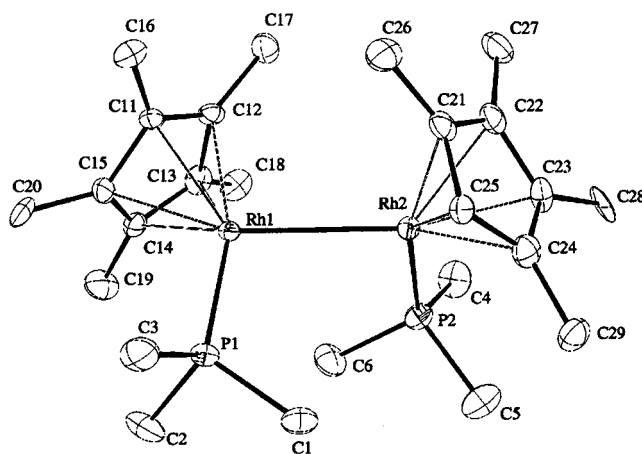


Figure 2. ORTEP diagram of $[(\text{Cp}^*(\text{PMe}_3)\text{Rh}(\text{H}))_2(\mu\text{-H})]^+$ (**3**, Hydride ligands were not located; BAR'_4^- counterion omitted for clarity).

issue. The iridium analogue of **3**, namely $[(\text{Cp}^*(\text{PMe}_3)\text{Ir}(\text{H}))_2(\mu\text{-H})]^+\text{X}^-$ ($\text{X} = \text{PF}_6$ or BF_4 , **14**), has been previously reported but was prepared using a dissimilar route.²³ The X-ray crystal structure of **14** shows that **3** and **14** are isostructural.

Activation parameters for the exchange of a terminal hydride with a bridging hydride have been reported for the iridium system, but determination of these parameters for the rhodium system is nontrivial.²³ Solubility of **3** becomes a problem at the low temperatures required to obtain well-resolved ^1H NMR spectra of the hydride signals. In addition, the numerous coupling interactions present make modeling of the exchange system difficult. Measurement of change in line widths with temperature provides an approximate free energy of activation of 9.1 ± 0.2 kcal/mol for exchange of terminal and bridging hydrides.

Characterization of **1 by NMR Spectroscopy.** In addition to resonances for Cp^* and PMe_3 , the ^1H NMR spectrum of **1** exhibits a doublet of doublets in the hydride region corresponding to three protons at -7.95 ppm (223 K; $^1J_{\text{Rh-H}} = 25$ Hz, $^2J_{\text{P-H}} = 11$ Hz). Recording a $^1\text{H}\{^31\text{P}\}$ NMR spectrum of **1** results in simplification of the hydride resonance to a doublet ($^1J_{\text{Rh-H}} = 25$ Hz). Additionally, a ^31P NMR spectrum obtained with decoupling of methyl protons reveals a quartet ($^2J_{\text{P-H}} = 11$ Hz). The hydride signal for all three spectra remains unchanged at all accessible temperatures (down to 123 K using a 750 MHz NMR spectrometer), suggesting that all three “hydride” ligands are equivalent on the NMR time scale.

Exposure of a solution of **1** to one atmosphere of D_2 gas results in partial deuteration of the hydride sites, producing a mixture of **1**, **1-d**₁, and **1-d**₂. These isotopomers exhibit distinct resonances in the ^1H NMR spectrum, as shown in Figure 3. At 223 K, an upfield isotope shift of 31 ppb with $J_{\text{H-D}} = 10.3$ Hz was observed for **1-d**₁, while a greater upfield shift of 121 ppb with $J_{\text{H-D}} = 9.9$ Hz was observed for **1-d**₂. These isotope shifts are temperature-dependent, with the shift difference between **1** and **1-d**₂ increasing to 137 ppb upon lowering the temperature to 180 K. Figure 4 shows the temperature dependence of the hydride chemical shifts for all three isotopomers.

Partial tritiation gives similar results, with upfield isotope shifts for **1-t**₁ and **1-t**₂ of 13 and 230 ppb, respectively, as observed by $^1\text{H}\{^31\text{P}\}$ NMR spectroscopy. Also observed are $J_{\text{H-T}}$ values of 72.8 Hz for **1-t**₁ and 66.8 Hz for **1-t**₂ (Figure 5). The isotope shift for **1-t**₂ increases as the temperature is lowered in a fashion similar to that in the partial deuteration results

(32) Werner, H.; Wolf, J. *Angew. Chem., Int. Ed. Engl.* **1982**, *21*, 296.

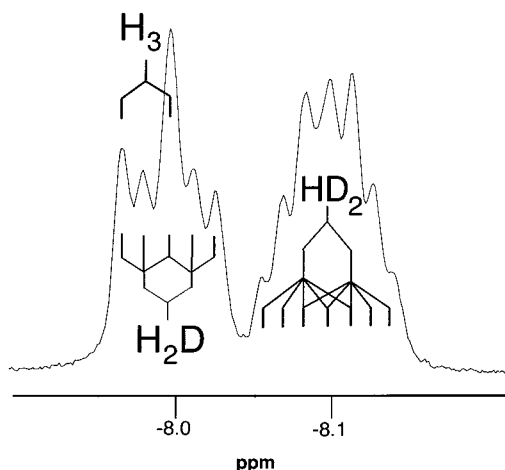


Figure 3. Partial (hydride region) 750 MHz $^1\text{H}\{^{31}\text{P}\}$ NMR spectrum of a mixture of complexes **1**, **1-d₁**, and **1-d₂** in CD_2Cl_2 at 223 K.

above. Table 2 summarizes the NMR data for all the isotopomers discussed above.

Determination of Hydride/Dihydrogen Structure of 1. As stated previously, the spectroscopic data are consistent with the presence of three equivalent “hydride” ligands in complex **1**. This observation may result from a fluxional hydride/dihydrogen structure as was observed for related cationic tris-pyrazolylborate complexes of Ir and Rh of the form $[\text{Tp}(\text{PMe}_3)\text{M}(\text{H})(\text{H}_2)]^+$ ($\text{M} = \text{Rh}, \text{Ir}$).^{13,20} Alternatively, the ground-state structure of **1** could be a dynamic trihydride, as reported for the closely related Ir complexes $[\text{Cp}(\text{PMe}_3)\text{Ir}(\text{H})_3]^+$ and $[\text{Cp}^*(\text{PMe}_3)\text{Ir}(\text{H})_3]^+$.^{18,23,24} These two possibilities can be distinguished with confidence by employing a combination of techniques: measurement of the relaxation rate of the hydride protons and analysis of the effect of partial substitution of the hydride ligands with deuterium or tritium.

The measurement of T_1 values for the hydride resonance in complex **1** was performed at temperatures between 240 and 130 K. The T_1 value decreases to a minimum of 23 ms at 150 K (500 MHz). This short $T_1(\text{min})$ value observed for the hydride ligands in complex **1** is qualitatively consistent with the presence of a bound dihydrogen ligand in a hydride/dihydrogen structure. The H–H bond length can be estimated from the mutual dipole–dipole relaxation rate R_{d-d} of the ^1H nuclei in the $\eta^2\text{-H}_2$ ligand ($R_{d-d} = 1/T_{1(d-d)}$). The total relaxation rate R_{H_2} is the sum of R_{d-d} and other relaxation rates from interaction with other magnetic dipoles in the complex, R_o ($R_{\text{H}_2} = R_{d-d} + R_o$).¹³ In the case of **1**, the R_{obs} ($T_1(\text{min})$) value is the weighted average of the relaxation rates of an ^1H in all sites. Thus, $R_{\text{obs}}(\mathbf{1}) = (2R_{\text{H}_2} + R_{\text{H}})/3$ where R_{H_2} and R_{H} are relaxation rates of the $\eta^2\text{-H}_2$ and terminal hydride ligands, respectively. We assume that R_{H} is modeled by the relaxation rate $R_{\text{obs}}(\mathbf{5})$ of the hydride ligand in the aquo complex **5** ($T_1(\text{min})$ of **5** = 1.3 s at 178 K, 500 MHz), and further, that this rate also approximates R_o . Therefore, as previously derived,¹³

$$R_{\text{obs}}(\mathbf{1}) = (2R_{\text{H}_2} + R_{\text{H}})/3 = [2(R_{d-d} + R_o) + R_{\text{H}}]/3 = [2R_{d-d} + 3R_{\text{obs}}(\mathbf{5})]/3$$

$$R_{d-d} = 3[R_{\text{obs}}(\mathbf{1}) - R_{\text{obs}}(\mathbf{5})]/2$$

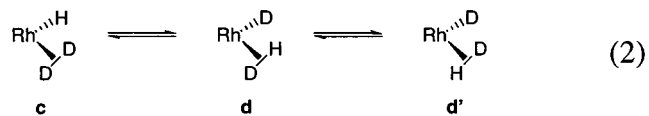
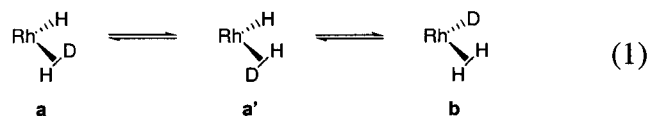
Using the experimental values reported above, $R_{d-d} = 64 \text{ s}^{-1}$.

Applying the method of Halpern, the H–H bond length can be bracketed between 0.82 Å (fast $\eta^2\text{-H}_2$ rotation) and 1.03 Å (slow rotation).^{33,34} A second method based on measurement of $J_{\text{H-D}}$ in the $\eta^2\text{-HD}$ ligand is described below which yields a more precise value for the H_2 bond length.

Partial deuteration of the hydride ligands in complex **1** leads to the observation of distinct resonances for **1**, **1-d₁**, and **1-d₂** in the ^1H NMR spectrum, with the deuterated species exhibiting substantial H–D coupling. The resonances due to **1-d₁** and **1-d₂** are shifted modestly upfield from that due to **1**. The chemical shift of the resonance due to **1-d₂** is temperature-dependent, with larger upfield shifts observed at lower temperature (Figure 4). At 223 K, the H–D coupling in **1-d₁** is 10.3 Hz, while the H–D coupling in **1-d₂** is 9.9 Hz. These values for $J_{\text{H-D}}$ are indicative of the presence of a dihydrogen ligand. If the deuterium atoms were distributed statistically in a hydride/dihydrogen structure, then $J_{\text{H-D}}$ would be approximately 30 Hz. The observation of temperature-dependent chemical shift differences and different values of $J_{\text{H-D}}$ in the different isotopomers are characteristic of isotopic perturbation of an equilibrium and a nonstatistical distribution of deuterium.

As previously reported for the iridium hydride/dihydrogen complex, the observed chemical shifts and $J_{\text{H-D}}$ coupling data can be analyzed quantitatively to calculate the limiting chemical shifts of the dihydrogen ligand (δ_{H_2}) and the terminal hydride ligand (δ_{H}), $J_{\text{H-D}}$ for the $\eta^2\text{-HD}$ ligand, and the energy difference which arises from deuterium substitution at the dihydrogen site versus the hydride site.¹³ In the case of complex **1**, this analysis is complicated by the relatively small isotope effects observed upon deuteration, which are similar in magnitude to the intrinsic isotope effects on the hydride chemical shifts resulting from partial deuteration.

The chemical shift of the H_3 isotopomer (δ_{H_3}) is simply the statistical average of the dihydrogen site and the hydride site, thus $\delta_{\text{H}_3} = (2\delta_{\text{H}_2} + \delta_{\text{H}})/3$. However, upon substitution of one deuterium atom in the hydride positions an equilibrium between three different species is obtained (eq 1). A similar equilibrium is obtained if two deuterium atoms are incorporated in the hydride positions (eq 2).



In this analysis we assume that there is no energy difference between structures **a** and **a'**. We also assume that the chemical shift of the *exo* hydrogen atom in **a** is the same as the *endo* hydrogen atom in **a'**. Also let a , a' , and b be the mole fractions of each species, so $a + a' + b = 2a + b = 1$. The Boltzmann factor A_1 , defined as $e^{-\Delta E/RT}$, may be introduced to account for an energy difference between **a** (or **a'**) and **b**. A_1 is equal to b/a

(33) Desrosiers, P. J.; Cai, L.; Lin, Z.; Richards, R.; Halpern, J. *J. Am. Chem. Soc.* **1991**, *113*, 4173.

(34) For a discussion and early analysis of fast vs slow $\eta^2\text{-H}_2$ rotation, see: Bautista, M. T.; Earl, K. A.; Maltby, P. A.; Morris, R. H.; Schweitzer, C. T.; Sella, A. *J. Am. Chem. Soc.* **1988**, *110*, 7031.

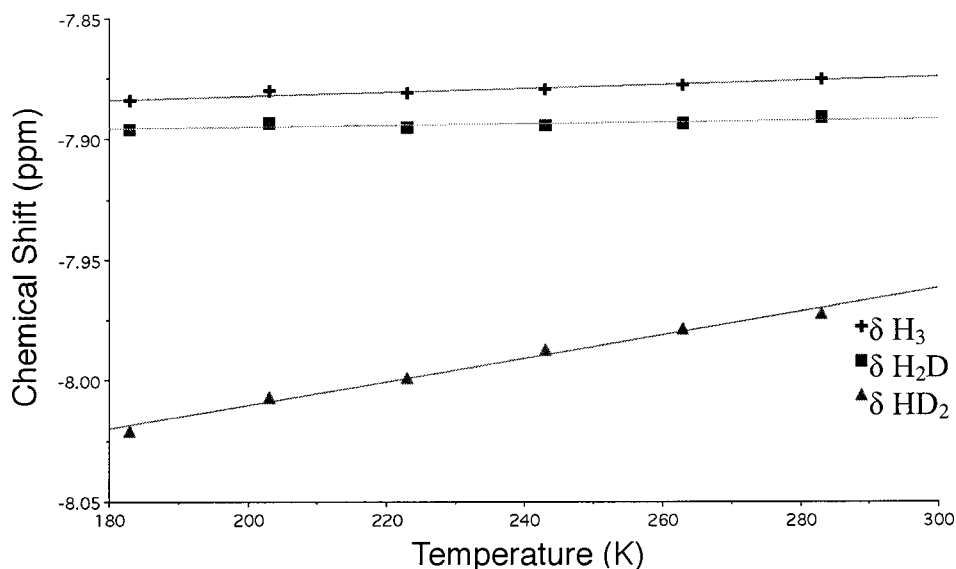


Figure 4. Chemical shifts for the hydride resonances in a mixture of **1**, **1-d₁**, and **1-d₂** as a function of temperature.

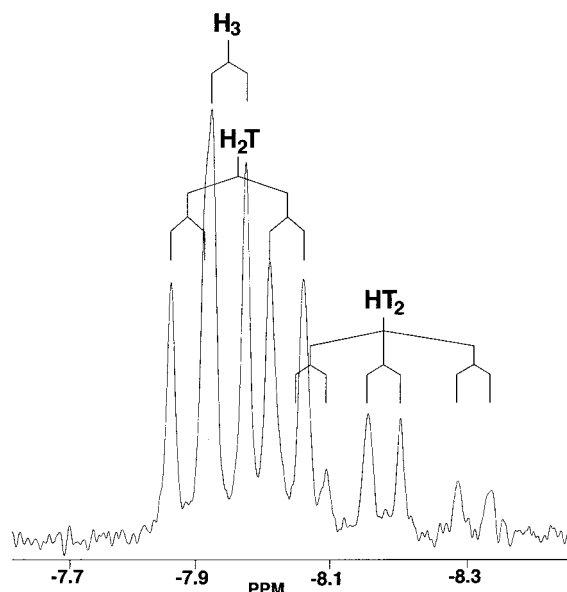


Figure 5. Partial (hydride region) 500 MHz $^1\text{H}\{^{31}\text{P}\}$ NMR spectrum of a mixture of complexes **1**, **1-t₁**, and **1-t₂** in CD_2Cl_2 at 223 K.

Table 2. Proton NMR Data for Various Isotopomers of Complex **1** at 223 K

	H ₃	H ₂ D	HD ₂	H ₂ T	HT ₂
δ (ppm) ^a	-7.95	-7.96 (31)	-8.09 (121)	-7.96 (13)	-8.10 (230)
$J_{\text{Rh-H}}$ (Hz)	24.8 ± 0.2	23.8 ± 0.2	22.1 ± 0.2	25.5 ± 0.2	23.8 ± 0.2
$J_{\text{H-D}}$ or $J_{\text{H-T}}$ (Hz)	—	10.3 ± 0.2	9.9 ± 0.2	72.8 ± 0.1	66.8 ± 0.1
$J_{\text{P-H}}$ (Hz)	9.8 ± 0.2	10 ± 0.2	10 ± 0.2	9.8 ± 0.2	9.6 ± 0.2

^a The chemical shifts are given in ppm, with the isotope shifts (ppb).

$= b/a'$. Thus, a and a' can be combined, and the mole fractions can be rewritten in terms of the Boltzmann factor, A_1 . For this case $a = a' = 1/(2 + A_1)$ and $b = A_1/(2 + A_1)$, leading to eq 3, as derived previously.¹³

$$\delta_{(\text{H}_2\text{D})} = \frac{\delta_{\text{H}_2} + \delta_{\text{H}} + A_1\delta_{\text{H}_2}}{2 + A_1} \quad (3)$$

This analysis excludes the contribution to the chemical shift of

intrinsic isotope effects (see below). In a similar fashion the observed $J_{\text{H-D}}$ coupling constant is given by eq 4, if the two-bond $^2J_{\text{H-D}}$ coupling between the dihydrogen ligand and the terminal hydride ligand is assumed to be zero.

$$J_{(\text{H}_2\text{D})} = \frac{^1J_{\text{H-D}}}{2 + A_1} \quad (4)$$

Similarly, expressions can be derived which relate the chemical shift and observed $J_{\text{H-D}}$ coupling of the HD₂ isotopomer, written in terms of a second Boltzmann factor, A_2 , where $A_2 = d/c$.

$$\delta_{\text{HD}_2} = \frac{2A_2\delta_{\text{H}_2} + \delta_{\text{H}}}{2A_2 + 1} \quad (5)$$

$$J_{(\text{HD}_2)} = \frac{^1J_{\text{H-D}}A_2}{2A_2 + 1} \quad (6)$$

Qualitatively, the observation that the H–D coupling constant in complex **1-d₁** is slightly greater than in **1-d₂** is consistent with some concentration of deuterium in the dihydrogen ligand, rather than the hydride site. Since the difference in the $J_{\text{H-D}}$ values is only slightly larger than the uncertainty in the measurements, we sought to verify this situation by measuring the H–T coupling constants in partially tritiated samples of **1**. By use of the ratio $\gamma_{\text{T}}/\gamma_{\text{D}} = 6.9465$, the $J_{\text{H-T}}$ value observed in **1-t₁** of 72.8 Hz can be converted to the more familiar $J_{\text{H-D}} = 10.5$ Hz, in good accord with the value of $J_{\text{H-D}} = 10.3$ Hz observed in **1-d₁**. The agreement of these coupling constants and the temperature-independent chemical shift of **1-d₁** suggest that the heavy isotope is distributed statistically in **1-d₁** and **1-t₁** (i.e., a/b and $A_1 \cong 1$) and that the true value for $^1J_{\text{H-D}}$ is ca. 31 Hz. These observations also suggest that the small and temperature invariant isotope shift of ca. 30 ppb observed in **1-d₁** is due to an intrinsic isotope effect.

In contrast, the isotope shift observed for **1-d₂** is large and temperature-dependent, consistent with the isotopic perturbation of the equilibrium in eq 2 (i.e., a/b and $A_2 \neq 1$). The value of A_2 can be estimated as 0.88 at 233 K from eq 6, knowing that $^1J_{\text{H-D}}$ is ca. 31 Hz and that the observed value for $J_{\text{H-D}}$ in **1-d₂**

is 9.9 Hz. It can be reasonably assumed that the intrinsic isotope effect contributing to the chemical shift in **1-d₂** is approximately 60 ppb, or roughly double the value observed in **1-d₁**. Values of A_2 at various temperatures can be calculated from the observed values of J_{H-D} in **1-d₂** and the chemical shift for the dihydrogen and hydride ligands in **1** can be deduced using eq 5. The values of A_2 obtained vary from 0.77 at 183 K to 0.91 at 243 K. The calculated chemical shifts are $\delta_{H_2} = -7.0$ ppm and $\delta_H = -9.6$ ppm. In light of the numerous approximations made above, a realistic uncertainty in these chemical shift values is ± 0.5 ppm.

These chemical shifts are not directly available by low temperature observation, since the rate of hydrogen atom exchange in **1** is too fast to allow for the observation of a static spectrum, even at 123 K. Using the chemical shifts derived above and the fact that a single resonance was observed at 123 K, a maximum activation energy of ca. 5 kcal/mol can be calculated for the dynamic process, indicating that the strong H–H bond in the bound dihydrogen ligand is being broken very rapidly.³⁵

An interesting aspect of these observations is that $A_1 \neq A_2$. This can be rationalized by noting that the relative energy of the isotopomers depicted in eq 1 and 2 is proportional to the reduced mass of the hydrogen (deuterium) atoms bound to the rhodium center. Substitution of deuterium for hydrogen in the hydride site will change the oscillator energy by $\sqrt{1/2}$, independent of any isotope substitution in the dihydrogen ligand. In contrast, the reduced mass varies with isotope substitution in a nonlinear fashion in the bound dihydrogen ligand. This leads to the observation that replacement of a second hydrogen atom with deuterium in the bound dihydrogen ligand has a greater effect than replacing the first one.

Using the well-known inverse correlation between the H–H bond length and the value of $^1J_{H-D}$, an H–H bond distance of 0.90 Å in the dihydrogen ligand of complex **1** can be derived.^{36–39} This suggests that neither of the two distances calculated above from the relaxation data are correct. The rate of rotation of the dihydrogen ligand in **1** may be intermediate between the fast and slow regime.⁴⁰

The value of $^1J_{H-D}$ derived here (and thus the H–H distance) is based on the assumption that the two-bond coupling between the bound dihydrogen and the adjacent hydride is zero. Coupling between bound dihydrogen and a hydride ligand has been observed in cases where the dihydrogen and hydride ligands are trans to each other.⁴¹ In one report⁴² of significant coupling between bound dihydrogen and a cis hydride ligand, this coupling is thought to arise from quantum mechanical exchange coupling, which would be quenched upon partial deuteration.

In the analysis of the ¹H NMR spectra of partially deuterated samples of complex **1**, the assumption of negligible H–D coupling between bound dihydrogen and adjacent hydride is reasonable.

Summary

The cationic Rh(III) complex $[\text{Cp}^*(\text{PMe}_3)\text{Rh}(\text{Me})(\text{CH}_2\text{Cl}_2)]^+\text{BAR}'_4^-$ (**4**) was prepared via chloride abstraction from $\text{Cp}^*(\text{PMe}_3)\text{Rh}(\text{Me})(\text{Cl})$ (**11**) using NaBAR'_4 in CH_2Cl_2 . Hydrogenolysis of **4** yielded $[\text{Cp}^*(\text{PMe}_3)\text{Rh}(\text{H})(\text{H}_2)]^+\text{BAR}'_4^-$ (**1**) for which the hydride resonance exhibits a single chemical shift down to 123 K at 750 MHz. The identification of **1** as a fluxional hydride/dihydrogen complex was made using T_1 , J_{H-D} , and J_{H-T} measurements. The interchange of hydride with dihydrogen sites must have a barrier (ΔG^\ddagger) less than ca. 5 kcal/mol.

Protonation of $\text{Cp}^*(\text{PMe}_3)\text{Rh}(\text{H})_2$ (**2**) with 1 equiv of $\text{H}(\text{OEt}_2)_2\text{BAR}'_4$ yielded a mixture of **1** and binuclear complex $[(\text{Cp}^*(\text{PMe}_3)\text{Rh}(\text{H}))_2(\mu\text{-H})]^+\text{BAR}'_4^-$ (**3**). Use of 0.5 equiv of acid resulted in clean formation of **3**, which was formulated as a fluxional bridging hydride complex based upon ¹H NMR spectroscopy and an X-ray structure determination. A free energy of activation of 9.1 kcal/mol was measured for exchange of terminal and bridging hydrides.

Experimental Section

General Considerations. Unless otherwise noted, all reactions and manipulations were performed using standard high-vacuum, Schlenk, or drybox techniques. Argon and nitrogen were purified by passage through columns of BASF R3-11 catalyst (Chemalog) and 4 Å molecular sieves. ¹H and ¹³C NMR chemical shifts were referenced to residual ¹H and ¹³C NMR signals of the deuterated solvents, respectively. ³¹P NMR chemical shifts were referenced to an 85% H_3PO_4 sample used as an external standard. Tritium NMR spectra were obtained at 533 or 800 MHz and externally referenced to CHDTCO_2^- .⁴³ The procedures for the safe storage and manipulation of tritium gas have been described previously.²⁴ Elemental analyses were performed by the University of California, Berkeley Microanalytical Facility, or by Atlantic Microlab Inc. of Norcross, GA. Mass spectrometric analyses were performed by the University of California, Berkeley Mass Spectrometry Facility.

Materials. All solvents were deoxygenated and dried via passage over a column of activated alumina.^{44,45} Deuterated solvents (Cambridge Isotope Laboratories) were purified by vacuum transfer from CaH_2 and stored over 4 Å molecular sieves. Compressed H_2 gas was purchased from Aldrich, D_2 from Matheson, and T_2 from American Radiolabeled Chemical, and all were used without further purification. NaBAR'_4 was purchased from Boulder Scientific and used without further purification. $\text{H}(\text{OEt}_2)_2\text{BAR}'_4$ was synthesized as described in the literature.⁴⁶ A 1.5 M solution of MeLi in Et_2O was purchased from Acros and used without further purification.

Complex **2** was initially reported by Maitlis but was prepared according to procedures published by Bergman.^{27,47} Complexes **9** and **11** have been previously reported and were synthesized according to literature procedures.^{30,31} Complex **8** is also known but was prepared using a method different from that reported in the literature (see below).²⁹ All spectroscopic data for the above compounds are in accord with published values.

- (35) For examples in the determination of H/H₂ exchange barriers and H–H bond distances using inelastic neutron scattering spectroscopy, see: (a) Eckert, J.; Albinati, A.; Bucher, U. E.; Venanzi, L. M. *Inorg. Chem.* **1996**, *35*, 1292. (b) Li, S.; Hall, M. B.; Eckert, J.; Jensen, C. M.; Albinati, A. *J. Am. Chem. Soc.* **2000**, *122*, 2903.
- (36) Maltby, P. A.; Schlaf, M.; Steinbeck, M.; Lough, A. J.; Morris, R. H.; Klooster, W. T.; Koetzle, T. F.; Srivastava, R. C. *J. Am. Chem. Soc.* **1996**, *118*, 5396.
- (37) Heinekey, D. M.; Luther, T. A. *Inorg. Chem.* **1996**, *35*, 4396.
- (38) Luther, T. A.; Heinekey, D. M. *Inorg. Chem.* **1998**, *37*, 127.
- (39) Grundemann, S.; Limbach, H. H.; Buntkowsky, G.; Sabo-Etienne, S.; Chaudret, B. *J. Phys. Chem. A* **1999**, *103*, 4752.
- (40) Morris, R. H.; Wittebort, R. J. *Magn. Reson. Chem.* **1997**, *35*, 243.
- (41) Bianchini, C.; Moneti, S.; Peruzzini, M.; Vizza, F. *Inorg. Chem.* **1997**, *36*, 5818.
- (42) Guari, Y.; Sabo-Etienne, S.; Chaudret, B. *J. Am. Chem. Soc.* **1998**, *120*, 4228.

- (43) Evans, E. A.; Warrell, D. C.; Elvidge, J. A.; Jones, J. R. *Handbook of Tritium NMR Spectroscopy and Applications*; Wiley: New York, 1985.
- (44) Pangborn, A. B.; Giardello, M. A.; Grubbs, R. H.; Rosen, R. K.; Timmers, F. J. *Organometallics* **1996**, *15*, 1518.
- (45) Alaimo, P. J.; Peters, D. W.; Arnold, J.; Bergman, R. G. *J. Chem. Educ.* **2001**, *78*(1), 64.
- (46) Brookhart, M.; Grant, B.; Volpe, A. F., Jr. *Organometallics* **1992**, *11*, 3920.
- (47) Periana, R. A.; Bergman, R. G. *J. Am. Chem. Soc.* **1986**, *108*, 7332.

Spectral Data for BAR'_4 . The ^1H and ^{13}C NMR resonances of the BAR'_4 ($\text{Ar}' = 3,5\text{-C}_6\text{H}_3(\text{CF}_3)_2$) counteranion in CD_2Cl_2 were essentially invariant for all cationic complexes discussed here, and spectroscopic data are not repeated for each compound. ^1H NMR (400 MHz, CD_2Cl_2) δ 7.73 (s, 8 H, H_o), 7.57 (s, 4 H, H_p). $^{13}\text{C}\{^1\text{H}\}$ NMR (101 MHz, CD_2Cl_2) δ 161.9 (q, $^1J_{\text{C-B}} = 49.8$, C_{ipso}), 135.0 (s, C_o), 129.0 (q, $^2J_{\text{C-F}} = 31.4$, C_m), 124.7 (q, $^1J_{\text{C-F}} = 272.6$, CF_3), 117.7 (s, C_p).

$[\text{Cp}^*(\text{PMe}_3)\text{Rh}(\text{H})(\text{H}_2)]^+\text{BAR}'_4^-$ (1**).** Solutions of complex **1** were generated using the following three procedures. (a) An NMR tube was charged with 5 mg (0.016 mmol) of **2** and sealed with a septum. The tube was placed in a 233 K bath, and a solution of $\text{H}(\text{OEt}_2)_2\text{BAR}'_4$ (32.0 mg, 0.032 mmol) in CD_2Cl_2 (0.5 mL) was added slowly via syringe. The contents of the tube were allowed to warm briefly (2–3 min) to room temperature and then cooled again in the 233 K bath. A ^1H NMR spectrum of the product revealed a mixture of approximately 90% **1** and 10% **3**. (b) A J-Young NMR tube was charged with a solution of **4** (5–10 mg of **4** in 0.5 mL CD_2Cl_2), sealed, and attached to a vacuum line. The sample was subjected to 4 freeze–pump–thaw cycles and placed in a 233 K bath. The sample was then exposed to ~ 1 atm H_2 , the NMR tube was sealed, and complex **1** was formed by vigorous shaking of the NMR tube. (c) In a third approach, 0.5 mL of CD_2Cl_2 or CDFCl_2 was vacuum-transferred into a 5-mm NMR tube containing 1–3 mg of **4**. Upon thawing to 233 K the solution was exposed to 1 atm H_2 for several min to afford **1**. The NMR tube was then sealed under ~ 500 Torr of H_2 gas. As mentioned previously, **1** could not be isolated due to rapid decomposition upon removal of solvent. However, solutions of **1** can be stored for long periods of time in a sealed vessel at 195 K or below. ^1H NMR (400 MHz, CD_2Cl_2 , 223 K) δ 1.92 (d, $^4J_{\text{P-H}} = 2.7$ Hz, 15 H, Cp^*), 1.42 (d, $^2J_{\text{P-H}} = 11.2$ Hz, 9 H, PMe_3), -7.95 (dd, $^1J_{\text{Rh-H}} = 24.6$ Hz, $^2J_{\text{P-H}} = 10.7$ Hz, 3 H, averaged H and $\eta^2\text{-H}_2$). $^{31}\text{P}\{^1\text{H}\}$ NMR (162 MHz, CD_2Cl_2 , 223 K) δ 5.6 (d, $^1J_{\text{Rh-P}} = 122.8$ Hz, PMe_3). $^{13}\text{C}\{^1\text{H}\}$ NMR (101 MHz, CD_2Cl_2 , 223 K) δ 104.1 (s, $\text{Cp}^*\text{-Ar}$), 19.2 (d, $^1J_{\text{C-P}} = 36.6$ Hz, PMe_3), 10.4 (s, $\text{Cp}^*\text{-Me}$).

Deuterium and Tritium Substitution in **1 (**1-d₁**, **1-d₂**, **1-t₁**, and **1-t₂**).** Deuterium was incorporated by freezing an NMR tube containing a solution of **1**, removing the H_2 atmosphere, and replacing it with D_2 gas. The NMR tube was then sealed under ~ 500 Torr D_2 gas. Tritiated samples were obtained by exposing solutions of **1** to 150 Torr T_2 at -40 °C for 20–60 min, yielding 20–60% tritiation or 15–40 mCi of activity. The apparatus for the safe manipulation of tritium has been previously described.²⁴ The samples were then frozen, the T_2 was removed, and the tube flame was sealed under vacuum.

$[(\text{Cp}^*(\text{PMe}_3)\text{Rh}(\text{H}))(\mu\text{-H})]^+\text{BAR}'_4^-$ (3**).** A Schlenk flask was charged with 50.0 mg (0.158 mmol) of **2** and placed in a 233 K bath. A cold (233 K) solution of $\text{H}(\text{OEt}_2)_2\text{BAR}'_4$ (80.0 mg, 0.079 mmol) in CH_2Cl_2 (4 mL) was cannula-transferred to the flask and the mixture allowed to warm to room temperature. The orange solution was stirred for 15–20 min and pentane (~ 1 mL) was added via syringe. The flask was placed in a freezer (243 K), and orange crystals of **3** (62.6 mg, 0.042 mmol, 53% yield) were isolated after a few days. ^1H NMR (400 MHz, CD_2Cl_2 , 193 K) δ 1.81 (s, 15 H, Cp^*), 1.27 (d, $^2J_{\text{P-H}} = 10.0$ Hz, 9 H, PMe_3), -14.91 (br s, 2 H, terminal H's), -21.33 (br s, 1 H, bridging H). ^1H NMR (400 MHz, CD_2Cl_2 , 253 K) δ 1.90 (d, $^4J_{\text{P-H}} = 2.8$ Hz, 15 H, Cp^*), 1.37 (d, $^2J_{\text{P-H}} = 10.1$ Hz, 9 H, PMe_3), -16.99 (br s; averaged signal for exchanging terminal and bridging H's). ^1H NMR (400 MHz, CD_2Cl_2 , 313 K) δ 1.95 (d, $^4J_{\text{P-H}} = 2.8$ Hz, 15 H, Cp^*), 1.43 (d, $^2J_{\text{P-H}} = 10.1$ Hz, 9 H, PMe_3), -16.99 (tt, $^1J_{\text{Rh-H}} = 14.4$ Hz, $^2J_{\text{P-H}} = 20.0$ Hz, 3 H, signal for rapidly exchanging terminal and bridging H's). $^{31}\text{P}\{^1\text{H}\}$ NMR (162 MHz, CD_2Cl_2 , 253 K) δ 4.5 (d, $^1J_{\text{Rh-P}} = 137.4$ Hz, PMe_3). $^{13}\text{C}\{^1\text{H}\}$ NMR (101 MHz, CD_2Cl_2 , 253 K) δ 100.2 (s, $\text{Cp}^*\text{-Ar}$), 21.1 (d, $^1J_{\text{C-P}} = 34.1$ Hz, PMe_3), 11.6 (s, $\text{Cp}^*\text{-Me}$). Anal. Calcd for $\text{C}_{58}\text{H}_{63}\text{BF}_{24}\text{P}_2\text{Rh}_2$: C, 46.61; H, 4.25. Found: C, 46.49; H, 4.23.

$[\text{Cp}^*(\text{PMe}_3)\text{Rh}(\text{Me})(\text{CH}_2\text{Cl}_2)]^+\text{BAR}'_4^-$ (4**).** A Schlenk flask was charged with 100 mg (0.209 mmol) of **10** and 94 mg (0.220 mmol) of

NaBAR'_4 and sealed with a rubber stopper. The flask was placed in an ice bath, and 5 mL of CH_2Cl_2 was introduced via syringe. The contents of the flask were stirred for 10–15 min and then filtered through Celite supported by a glass frit. The filtrate was concentrated in vacuo and the flask placed in a freezer (243 K) for 2 d. Orange-red crystals of **4** (223 mg, 0.175 mmol) were isolated in 84% yield. Alternately, this procedure can be repeated using 75 mg (0.206 mmol) of **11** and 191 mg (0.216 mmol) of NaBAR'_4 to produce crystals of **4** (224 mg, 0.175 mmol) in 85% yield. ^1H NMR (400 MHz, CD_2Cl_2 , 273 K) δ 5.33 (s, CH_2Cl_2), 1.60 (d, $^4J_{\text{P-H}} = 2.6$ Hz, 15 H, Cp^*), 1.44 (d, $^2J_{\text{P-H}} = 10.1$ Hz, 9 H, PMe_3), 0.74 (d, $^3J_{\text{P-H}} = 6.7$ Hz, 3 H, Me). $^{31}\text{P}\{^1\text{H}\}$ NMR (162 MHz, CD_2Cl_2 , 273 K) δ 3.2 (d, $^1J_{\text{Rh-P}} = 163.6$ Hz, PMe_3). $^{13}\text{C}\{^1\text{H}\}$ NMR (101 MHz, CD_2Cl_2 , 273 K) δ 101.5 (s, $\text{Cp}^*\text{-Ar}$), 54.2 (s, CH_2Cl_2), 14.8 (d, $^1J_{\text{C-P}} = 32.1$ Hz, PMe_3), 9.4 (s, $\text{Cp}^*\text{-Me}$), 2.0 (dd, $^1J_{\text{C-Rh}} = 24.7$ Hz, $^2J_{\text{C-P}} = 14.4$ Hz, Me). Anal. Calcd for $\text{C}_{47}\text{H}_{41}\text{-BF}_{24}\text{Cl}_2\text{PRh}$: C, 44.19; H, 3.24. Found: C, 44.21; H, 3.27. FAB LRMS: m/z 329 $[(\text{Cp}^*(\text{PMe}_3)\text{Rh}(\text{Me}))]^+$.

$[\text{Cp}^*(\text{PMe}_3)\text{Rh}(\text{H})(\text{OH}_2)]^+\text{BAR}'_4^-$ (5**).** A trace amount of complex **5** was formed in the reaction to generate **1**. Residual H_2O present in the solvent and/or added H_2 gas served to displace the labile $\eta^2\text{-H}_2$ ligand from **1**, thereby forming **5**. ^1H NMR (400 MHz, CD_2Cl_2 , 223 K) δ 1.72 (s, 15 H, Cp^*), 1.45 (d, $^2J_{\text{P-H}} = 13.4$ Hz, 9 H, PMe_3), -9.63 (dd, $^1J_{\text{Rh-H}} = 20.4$ Hz, $^2J_{\text{P-H}} = 45.1$ Hz, 1 H, hydride).

$\text{Cp}^*(\text{PMe}_3)\text{Rh}(\text{Me})_2$ (8**).** In air, a Schlenk flask was charged with 200 mg (0.519 mmol) of **7** and sealed with a rubber stopper. The flask was evacuated and back-filled with Ar 4 \times , and 10 mL of dry, degassed Et_2O was added via syringe. While stirring, 1.56 mmol (1.0 mL of a 1.5 M solution of MeLi in Et_2O) of MeLi was added slowly via syringe. The contents of the flask were stirred for 12 h after which ~ 0.1 mL of H_2O was added to quench the MeLi. All liquids were cannula-filtered into another Schlenk flask, and the volatile materials were removed in vacuo to produce a brown solid. This solid was dissolved in pentane and filtered through alumina. The light orange filtrate was collected and the solvent removed in vacuo to produce **8** (114 mg, 0.332 mmol) in 64% yield. Complex **8** has been previously characterized, but was prepared using a different route.²⁹

$\text{Cp}^*(\text{PMe}_3)\text{Rh}(\text{Me})(\text{OTf})$ (10**).** A Schlenk flask was charged with 100 mg (0.290 mmol) of **8** and 178 mg (0.290 mmol) of **9** and sealed with a rubber stopper. The flask was placed in an ice bath, and 15 mL of Et_2O was introduced via syringe. The contents of the flask were allowed to warm to rt while stirring. After 12 h of stirring the brown-black solution was filtered through silanized silica gel and all solvent removed in vacuo from the filtrate to produce an orange-brown solid. This solid was recrystallized from Et_2O /pentane to produce **10** (181 mg, 0.378 mmol) in 65% yield. ^1H NMR (400 MHz, CD_2Cl_2 , rt) δ 1.60 (d, $^4J_{\text{P-H}} = 2.5$ Hz, 15 H, Cp^*), 1.45 (d, $^2J_{\text{P-H}} = 10.3$ Hz, 9 H, PMe_3), 0.83 (d, $^3J_{\text{P-H}} = 6.9$ Hz, 3 H, Me). $^{31}\text{P}\{^1\text{H}\}$ NMR (162 MHz, CD_2Cl_2 , RT) δ 6.7 (d, $^1J_{\text{Rh-P}} = 165.7$ Hz, PMe_3). ^{19}F NMR (376 MHz, CD_2Cl_2 , RT) δ -79.1 (s). $^{13}\text{C}\{^1\text{H}\}$ NMR (101 MHz, CD_2Cl_2 , RT) δ 119.7 (q, $^1J_{\text{C-F}} = 320.2$ Hz, CF_3), 98.5 (s, $\text{Cp}^*\text{-Ar}$), 14.6 (d, $^1J_{\text{C-P}} = 30.1$ Hz, PMe_3), 9.5 (s, $\text{Cp}^*\text{-Me}$), 4.2 (dd, $^1J_{\text{C-Rh}} = 22.3$ Hz, $^2J_{\text{C-P}} = 16.5$ Hz, Me).

Measurement of Activation Parameter Using NMR Line Broadening Techniques. The activation barrier for exchange of a terminal hydride with a bridging hydride in complex **3** was measured using standard NMR line broadening experiments conducted at temperatures between 163 and 223 K. Line widths (ν) were measured at half-height in units of Hz and were corrected for line widths (ν_o) at the low-temperature limit. The exchange rates were determined from the equation $k = \pi(\nu - \nu_o)$. Free energies of activation were calculated from the Eyring equation $\Delta G^\ddagger = -RT[\ln(kh/k_B T)]$.

Crystallographic Studies. Crystallographic studies were performed by Dr. Peter S. White (complex **3**) at the University of North Carolina, Chapel Hill, Single-Crystal X-ray Facility or by Dr. Frederick J. Hollander (complex **4**) at the University of California, Berkeley, X-ray Crystallography Facility.

For complex **3**, data were collected at 173 K on a Bruker SMART diffractometer, using the omega scan mode. The structure was solved by direct methods. Refinement was by full-matrix least squares with weights based on counter statistics. All non-hydrogen atoms were refined anisotropically, while H atoms were refined using a riding model. Crystal data and collection parameters are given in the Supporting Information. All computations were performed using the NRCVAX suite of programs.⁴⁸

For complex **4**, all measurements were made at 159 K on a Siemens SMART diffractometer with graphite monochromated Mo K α radiation. The structure was solved by direct methods and expanded using Fourier techniques. Hydrogen atoms were included in calculated positions but not refined. Data were integrated using the program SAINT and corrected for Lorentz and polarization effects.⁴⁹ No decay correction was applied. The data were analyzed using the program XPREP to determine space group and cell contents.⁵⁰ Crystal data and collection parameters are given in the Supporting Information.

Acknowledgment. Research performed in the M. S. B. laboratory at UNC was supported by the NSF (CHE-0107810). Research performed in the D. M. H. laboratory at UW was supported by the NSF (CHE-9807358). Acquisition of the 750 MHz NMR spectrometer was supported by the Murdoch Charitable Trust and the NSF. We acknowledge NSF support (CHE-9710008) of a 500 MHz spectrometer upgrade. The work done in the R. G. B. laboratory at UCB was supported by the Director, Office of Energy Research, Office of Basic Energy Sciences, Chemical Sciences Division, U.S. Department of Energy, under Contract No. DE-AC03-76SF00098.

Supporting Information Available: Crystallographic data for complexes **3** and **4** (CIF). This material is available free of charge via the Internet at <http://pubs.acs.org>.

JA0165990

(48) Gabe, E. J.; Le Page, Y.; Charland, J.-P.; Lee, F. L.; White, P. S. *J. Appl. Crystallogr.* **1989**, *22*, 384.

(49) SAINT: SAX Area-Detector Integration Program; Version 4.024; Siemens Industrial Automation, Inc., Madison, WI, 1995.

(50) XPREP: Version 5.03; Part of the SHELXTL Crystal Structure Determination Package; Siemens Industrial Automation, Inc., Madison, WI, 1995.